Universidad de Cádiz

Microgrid Cluster Energy Management with a PLC

Carrasco González, David; Sarrias Mena, Raúl; Horrillo Quintero, Pablo; Llorens Iborra, Francisco; De la Cruz Loredo, Iván; Ugalde Loo, Carlos Ernesto; Fernández Ramírez, Luis Miguel

Published in:
2025 5th International Conference on Electrical, Computer and Energy Technologies (ICECET)

DOI (link to publication from Publisher):
10.1109/ICECET63943.2025.11472221

Publication date:
2026

Document Version:
Camera ready

Citation for published version (IEEE):
D. Carrasco-González et al., "Microgrid Cluster Energy Management with a PLC," 2025 5th International Conference on Electrical, Computer and Energy Technologies (ICECET), pp. 1–6, Jul. 2025, doi: 10.1109/ICECET63943.2025.11472221.

979-8-3315-3559-9/25/$31.00 ©2025 IEEE

Microgrid Cluster Energy Management with a PLC

David Carrasco-González
SURET Research Group
Dept. Electrical Engineering
University of Cadiz
ETSI Algeciras, Spain
david.carrasco@uca.es

Raúl Sarrias-Mena
SURET Research Group
Dept. Engineering in Automation, Elec. and Comp. Arch. & Net
University of Cadiz
ETSI Algeciras, Spain
raul.sarrias@uca.es

Pablo Horrillo-Quintero
SURET Research Group
Dept. Electrical Engineering
University of Cadiz
ETSI Algeciras, Spain
pablo.horrillo@uca.es

Francisco Llorens-Iborra
SURET Research Group
Dept. Electrical Engineering
University of Cadiz
ETSI Algeciras, Spain
francisco.llorens@uca.es

Iván De la Cruz-Loredo
CIREGS
School of Engineering
Cardiff University
Cardiff, United Kingdom
DeLaCruzLoredoI@cardiff.ac.uk

Carlos E. Ugalde-Loo
CIREGS
School of Engineering
Cardiff University
Cardiff, United Kingdom
Ugalde-LooC@cardiff.ac.uk

Luis M. Fernández-Ramírez
SURET Research Group
Dept. Electrical Engineering
University of Cadiz
ETSI Algeciras, Spain
luis.fernandez@uca.es

***Abstract*—Microgrid clusters (MGCs) provide an opportunity for system operators to enhance efficiency, resilience, and reliability of energy systems. MGCs can combine direct current (DC) and alternating current (AC) technologies by integrating different power generation, consumption and storage technologies, thus offering flexibility and resilience to individual microgrids (MGs). However, verification of practical control systems for MGCs is required to ensure robustness and efficiency of the power dispatch. This work contributes to this effort by presenting, implementing and verifying a control system for an MGC. This MGC comprises separate DC and AC MGs interconnected to a local grid: the DC MG incorporates DC loads, a wind turbine, a fuel cell, an electrolyzer, and an ultracapacitor; and the AC MG comprises AC loads, an electrical battery bank, and a photovoltaic power plant. The control system uses a dynamic centralized energy management system (EMS) that coordinates power dispatch and energy distribution between all energy storage systems and local device controllers. The control system, specifically the EMS, is evaluated across different operating scenarios in an experimental validation environment composed of an OPAL-RT unit and a SIMATIC ET 200SP Open Controller PLC. The results show that the implemented EMS exhibits robust real-time behavior across different operating scenarios.**

Keywords—Energy management system, experimental validation, microgrid cluster, real-time operation and control.

I. Introduction

In recent years, the need for climate change mitigation has significantly increased the deployment of renewable energy sources. This situation has been accelerated by international agreements to decarbonize the energy sector by mitigating emissions and eliminating fossil fuels gradually [1]. At the same time, energy demand in cities and industries is growing significantly. One possible response to these challenges is the design of smaller and more autonomous grids known as microgrids (MGs). MGs offer advantages owing to their reduced emissions, enhanced energy reliability and quality, more economic operation, and increased energy efficiency [2].

MGs combine distributed loads, energy storage systems (ESSs), and renewable energy technologies (RETs) into controlled, self-contained entities with defined electrical limits [3]. Research has traditionally focused on alternating current (AC) MGs owing to their similarities with conventional electricity grids. However, there has been an increased interest in direct current (DC) MGs in recent years [4]. This flexibility allows MGs to operate using DC, AC, or hybrid DC/AC technologies, enabling greater flexibility and adaptability [5].

MGs offer flexibility in operation, enabling them to function independently in remote regions, where connecting to the main electricity grid is difficult [6]. MGs are often interconnected to the local grid via a point of common coupling (PCC). This connection enables two operational modes: islanded and grid-connected modes. In an islanded mode, the MG operates isolated from a main grid, relying solely on its internal generation and stored energy to meet local demand. Any excess or deficit in energy demand needs to be managed within the MG using its RETs or ESSs [7]. Conversely, in a grid-connected mode, the MG interacts with the main electricity grid, exchanging electricity as needed. The grid can supply additional electricity during periods of high demand within the MG or absorb any electricity surplus within the MG [8].

DC/AC technology integration and connection of an MG to the conventional electricity grid facilitates the interconnection of several adjacent MGs to constitute a microgrid cluster (MGC). This type of system configuration offers several advantages, such as enhanced overall performance, including

This work was partially supported by Ministerio de Ciencia e Innovación, Agencia Estatal de Investigación, FEDER, UE (Grant PID2021-123633OB-C32 supported by MCIN/AEI/10.13039/501100011033/FEDER, UE).

increased resilience, efficiency, reliability, and sustainability; localized energy balance, improving the grid stability and self-sufficiency of a community; and decentralized electrical power systems, reducing reliance in conventional grids and promoting local energy autonomy [9]. To achieve their control objectives, energy management systems (EMSs) are crucial for managing MGs. The primary function of the EMS is to generate operating setpoints to the energy sources of the MGs, and this can be realized through diverse methodologies discussed in [10], [11].

This work presents the experimental verification of a control system for a MGC that comprises separate DC and AC MG interconnected to a local electricity grid. The control system uses a dynamic centralized EMS is employed to coordinate power dispatch and energy distribution and local device controllers. The control system, specifically the EMS, is tested under fluctuating incident solar radiation and wind speed and dynamic loads conditions in an experimental validation environment composed of an OPAL-RT unit and a SIMATIC ET 200SP Open Controller PLC.

The paper is organized as follows. Section II describes the model used to represent the MGC. Section III describes the control system implemented in the MGC. The experimental verification of the control system is presented in Section IV. Section V presents and analyzes the experimental results. Finally, the conclusions of this work are presented in Section VI to close the paper.

II. Microgrid Cluster Configuration

The MGC under study incorporates an AC and DC MG, and a connection point to a local grid, as shown in Fig. 1. All elements of the MGC including RETs and ESSs are regulated independently to track control references. At a higher control level, a dynamic centralized EMS oversees the entire operation of the MGC, orchestrating the operation of all elements of the MGC. A detailed specification of each element of the system is presented in the subsequent subsections.

A. Alternating Current Microgrid

The AC MG comprises a photovoltaic (PV) power plant, local AC loads and a battery energy storage system (BESS). All these devices are interconnected in a three-phase AC bus rated at 600 V. This 600 V AC bus is also interconnected with the local grid and the DC MG through a PCC, forming the MGC.

The PV generator is modeled via series and parallel resistances, a parallel diode model and a current source [12]. The PV modules require a DC/DC boost converter, which increases the voltage for optimal PV power generation using a maximum power point tracking (MPPT) strategy. A 'perturb and observe' (P&O) algorithm determines the operating duty cycle for the boost converter for maximum PV power output. A voltage source inverter (VSI) ensures compatibility with the local electricity grid by regulating voltage and frequency. The inverter control is achieved using cascaded control loops based on proportional-integral (PI) controllers, which aim to maintain a constant DC voltage output of the boost converter [13].

The AC MG also incorporates a Li-Ion based BESS. The BESS is modeled as a resistor in series with a controlled voltage source, reproducing its electrical characteristic. The BESS is interconnected with the 600 V AC bus voltage of this MG via a VSI. Employing cascaded control loops, the VSI regulates the reactive and active power exchange between the MG and the BESS.

Two local three-phase inductive loads connected in a star configuration are considered in the AC MG. These loads are dynamically switched on and off across different time periods to emulate fluctuating energy demand within the AC MG.

B. DC Microgrid

The DC MG consists of two DC loads, ESSs, such as an ultracapacitor (UC) and hydrogen-based technologies including a fuel cell (FC) and an electrolyzer (EZ), and a wind tubine (WT). All components are linked via an 1100 V DC bus. The configuration of the DC MG is shown in Fig. 1.

A Type 4 WT based on a synchronous generator is considered. This has been modeled as a sixth-order system [14].

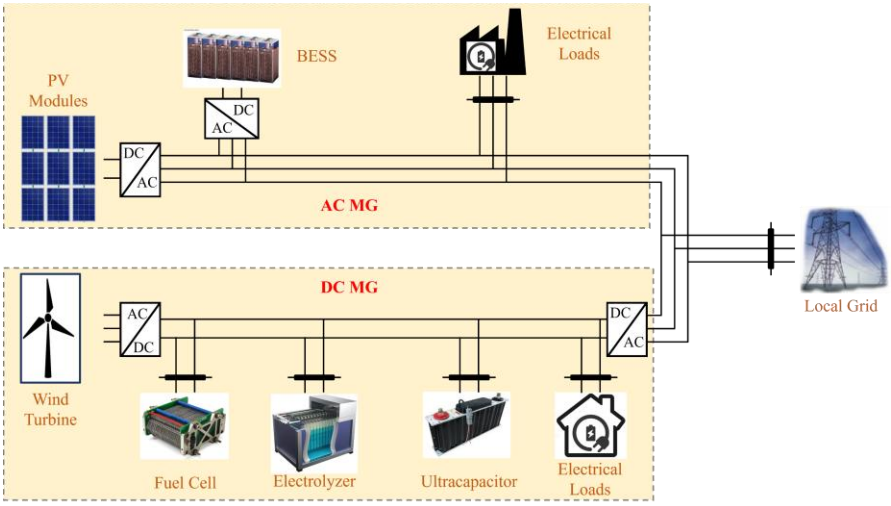

Fig. 1. Configuration of the MGC.

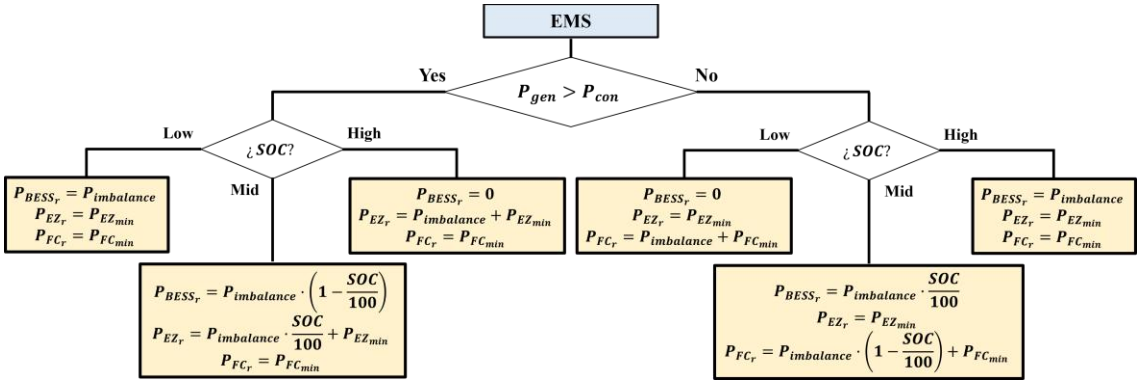

Fig. 2. Structure of the EMS.

The generator is connected to the 1100 DC bus via an uncontrolled bridge rectifier that converts the generated AC power into DC and a DC/DC boost converter that adapts the DC vo ltage levels and regulates WT speed. Such a configuration optimizes WT operation under fluctuating wind speeds.

A bidirectional half-bridge converter connected to the UC enables discharging and charging the UC and, thus, a two-way energy exchange. As an EZ always consumes electricity, a buck converter is used to connect the EZ to the 1100 V DC bus. Conversely, the FC utilizes a boost converter as it only injects power into the 1100 V DC bus. The UC is represented by a series resistor with an ideal capacitor. The FC is represented by a diode model and a controlled voltage source. The EZ modeled by a voltage source and a series resistance.

The local DC loads are directly connected to the MG, with controlled circuit breakers enabling their connection and disconnection.

A VSI acts as the interface between the 1100 V DC bus and the 600 V AC bus. It is used to convert DC into AC power compatible with the AC MG, ensuring a steady DC bus voltage despite power variations arising from the variable wind speed and changing loads within the DC MG.

C. Local Electricity Grid

The MGC connects to an strong AC local grid (i.e. an infinite bus) represented by a three-phase AC voltage source with negligible internal impedance and constant voltage (600 V) and frequency (60 Hz). This local electricity grid is interconnected with the AC MG via a PCC. The energy imbalance is inherently controlled to maintain frequency and voltage stability at the PCC. This automatic control eliminates the need for specific actions on the regulation of reactive and active power exchange with the local grid.

The MGC operates exclusively connected to the local electricity grid. The analysis of an islanded operation falls out of the scope of this paper.

III. Microgrid Cluster Control

A. Local Control

As mentioned earlier in the paper, for the PV generator, the P&O algorithm is utilized to enable an MPPT strategy and to optimize the power generation under varying solar irradiance. Similarly, the WT speed regulation ensures tracking of the optimal power curve based on the prevailing wind speed.

The active power transfer between each ESS and the MGC is regulated using PI controllers, which ensure active power exchange is in accordance to reference values provided by the EMS. The UC controller accepts both negative and positive control references, enabling both charging and discharging operations. The EZ controller only accepts negative control references, corresponding to power consumption. Conversely, the FC controller only accepts positive control references, signifying power injection into the system.

Finally, time-controlled circuit breakers manage the connection and disconnection of DC and AC local loads within each MG. The loads do not necessitate dedicated control strategies since their behavior is already accounted by the EMS.

B. Energy Management System

A dynamic centralized EMS was developed to oversee the operation of all elements of the MGC. The EMS uses a function based on ‘if-then’ statements to produce the setpoints of power for all the MGC ESSs to minimize power exchange with the electricity local grid and ensure the safety of the ESS by monitoring their state-of-charge (SOC), as depicted in Fig. 2. This type of EMS relies on defining different operational scenarios for the system, with each scenario representing a specific condition.

Power generation of RETs is combined into a single generation pool, and all the power required by the loads is combined into a single demand pool. The dynamic EMS operates at a high frequency update rate to ensure the energy balance within the system. When energy is not balanced, the ESSs compensate for the imbalance according to their availability. The BESS is used preferably based on its SOC, while the hydrogen system supports it to prevent the BESS from reaching very low or high SOC. In addition, the hydrogen system has a reduced power generation and power consumption level to avoid disconnection of the FC or EZ when operation of one of these devices is not required. The UC handles transient energy imbalances which other ESSs cannot manage owing to their slower response.

Based on the previous architecture, the EMS first calculates the difference between the generated and consumed power.

When the generated power exceeds the consumed power, the EMS directs the ESSs to store the excess energy. Conversely, when the consumed power exceeds the generated power, the EMS directs the ESSs to discharge power into the MGC. Next, the SOC of the BESS is assessed. If SOC is high (above 80%), the BESS is prevented from storing power, and the EZ handles the excess of power. If SOC is low (below 30%), the BESS is prevented from discharge, and the FC assists in meeting demand. If the SOC is within acceptable limits (between 30% and 80%), the hydrogen system (FC or EZ, as needed) and the BESS contribute to the energy balance in the MGC. As a final step, the active power refence of the UC is calculated as the control error among the power measured of the BESS, FC, and EZ and their respective setpoint values.

IV. Experimental Validation Environment

This section details the experimental environment used to verify the real-time performance of the proposed control system.

A. Structure of the Experimental Validation Environment

The structure of the environment to conduct the experimental verification, shown in Fig. 3, is mainly composed of an OPAL-RT unit, a Siemens programmable logic controller (PLC) and a personal computer (PC) host.

The OPAL-RT unit serves as a real-time simulator for hardware-in-the-loop (HIL) testing. The models of the MGC, created in MATLAB/Simulink, are implemented on this platform using the software RT-LAB. This software can manage model editing, building, loading, execution and monitoring. An OPAL-RT 4512 unit is used to implement and execute in real-time the MGC and its local controls.

A PLC is a programmable computer employed for automation and control processes in industrial environments. The control systems, created in MATLAB/Simulink, are implemented on this platform using the TIA Portal software. This software can make hardware configuration, program development, deployment of the program in the PLC, execution and monitoring. A SIMATIC ET 200SP Open Controller PLC from Siemens is used to implement and execute the dynamic centralized EMS.

The PC host executes Simulink (MATLAB), TIA Portal and the RT-LAB software. It also serves as the platform for system design and modeling within Simulink.

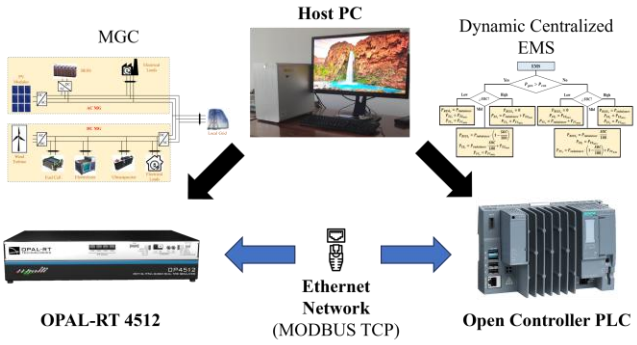

Fig. 3. Structure of the experimental validation environment.

The MGC and the local control, designed for real-time validation, are divided into three subsystems. A master subsystem contains the dynamic configuration of the MGC, while a slave subsystem contains the local control. These subsystems are introduced to the OPAL-RT unit via RT-LAB. The third subsystem provides visualization and monitoring of the MGC and control system response.

B. Communication System

OPAL-RT supports a variety of communication systems, enabling realistic real-time validations for industrial applications [15]. This provides greater flexibility for users, eliminating the need for additional components.

The Modbus transmission control protocol (TCP) is a well-established protocol for real-time communication in industrial and energy applications, owing to its comprehensive error-handling capabilities and robustness [16]. Modbus TCP operates over Ethernet. Thus, real-time data exchange between the OPAL-RT unit and the PLC is facilitated via an Ethernet network where each device is assigned a single IP address.

Communication in the experimental setup is carried out in two steps. First, the MGC transmits the generated and consumed power and the SOC of the BESS from the OPAL-RT unit to the PLC. Then, in the PLC, the EMS calculates the setpoints of power for all the MGC ESSs and sends these back to the OPAL-RT unit.

V. Experimental Results and Discussion

To assess the performance of the control approach for the MGC across under different operating scenarios, a 10-seconds test was carried out. These scenarios model fluctuating incident solar radiation and wind speeds to simulate variations in the PV and WT power generation. Solar radiation was modeled as a constant 900 W/m^2 from 0 to 6 s into the simulation, 400 W/m^2 from 6 to 8 s, and 200 W/m^2 from 8 to 10 s. On the other hand, wind speed was modeled as an 8.5 m/s mean from 0 to 5 s, and 12.5 m/s from 5 to 10 s. The resulting generated power from these input scenarios are shown in Fig. 4.

Both AC and DC local loads are dynamically connected and disconnected throughout the simulation. The DC loads, initially disconnected, include a 700 kW load that connects at 3 s and a 250 kW load that connects at 8 s. The AC local loads include a 1.8 MW/200 kVAr load that remains connected during the simulation, and a 700 kW/100 kVAr load that is connected from 4 to 7.5 s into the test. The initial SOC of the BESS was defined as 50%.

Fig. 4 shows the power exchange with the local electricity grid (P_{PCC}) and the generated and consumed power in the MGC. As depicted, the local grid interacts with the MGC to maintain the energy balance when there are changes in the inputs of the technologies that compound the MGC, such as fluctuating winds speed and incident solar radiation, and dynamic load conditions. In addition, it supplies or absorbs the energy deficit or surplus in the MGC that the ESSs cannot handle to maintain energy balance. When generation and demand are balanced again, the

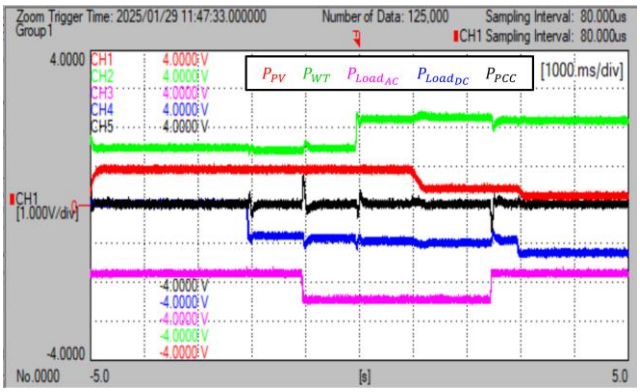

Fig. 4. Power exchange with the local grid and the generated and consumed power in the MGC.

power exchange with the local grid decreases to zero. This condition persists throughout most of the test, confirming the goal of minimizing local grid usage.

The variations in the PV and WT power generation observed in Fig. 4 are caused by the fluctuations in the winds speeds and incident solar radiation and wind speeds. Additionally, the dynamic variations in the loads are caused by the disconnection/connection of them into the AC and DC buses.

While both AC and DC local loads were represented by constant values, the DC load profile exhibits minor fluctuations. These variations in the DC local loads are produced by the voltage fluctuations in the DC bus. This phenomenon is undetectable in the AC load profile, attributed to the local grid constant voltage regulation on the AC bus. A similar situation occurs with the WT power generation.

Fig. 5 provides a good understanding of the generated and consumed power in the MGC without using ESSs to balance the energy. Power generation exceeds power consumption in the simulation intervals 0-2.5 s and 3.5-5 s. In contrast, power consumption exceeds power generation in the rest of the intervals of the test. This confirms the correct operation of the EMS, minimizing the reliance of the system on the local grid under the different power mismatches.

Fig. 6 presents the active power output of each ESS in the MGC and their corresponding control set-point values. The

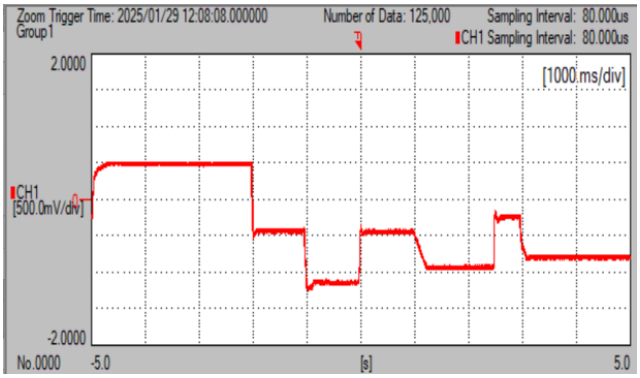

Fig. 5. Difference among the generated and consumed power in the MGC.

results show that all local controllers exhibit an acceptable performance, which confirms their effectiveness. When power generation exceeds power consumption, the EMS directs the ESSs to store the energy surplus of the MGC. Conversely, when power consumption exceeds power generation, the EMS directs the ESSs to discharge into the MGC.

The BESS stores or supplies energy at around half of its rated power due to the initial SOC. The hydrogen system supports the BESS, maintaining energy balance in the system and ensuring its proper usage.

The UC perfectly handles transient power mismatches with large peaks, as observed in Fig. 6. When the other ESSs reach a steady state, the UC power output returns near to zero.

Fig. 7 shows the voltage of the DC bus. This voltage is effectively regulated around its reference value (1,100 V). This precise control is indispensable for a stable operation of all DC MG technologies. While changes in the hydrogen system and UC operation, disconnection/connection of DC local loads, and WT generation cause voltage fluctuations, the local control of the VSI of the DC MG regulates effectively the DC bus voltage.

The results presented in this section show robust performance across the different testing scenarios, with appropriate responses from both the control system and the MGC.

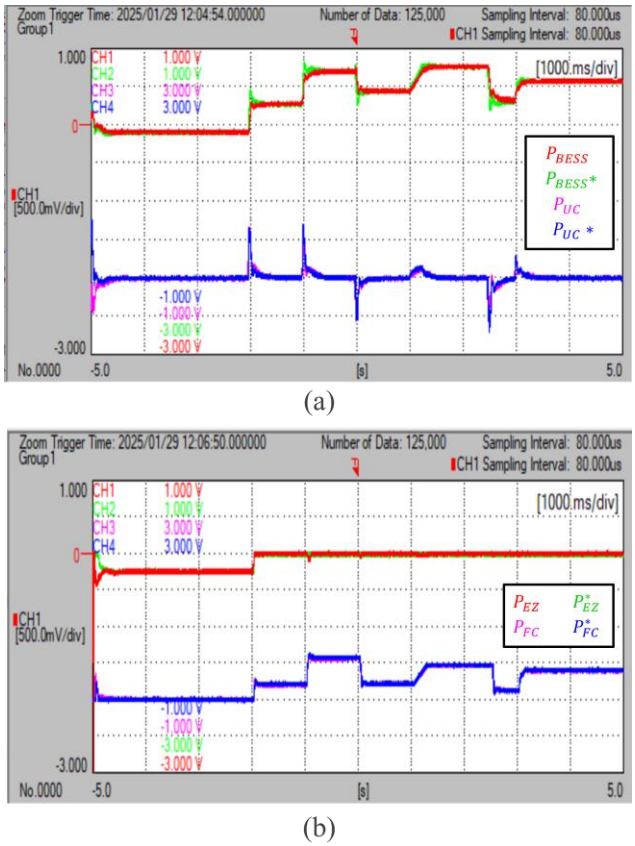

Fig. 6. Active power output of each ESS and their references: (a) BESS and UC, and (b) EZ and FC.

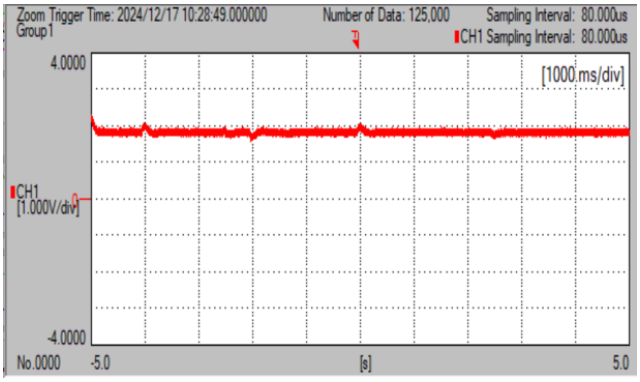

Fig. 7. Voltage of the DC bus evolution.

CONCLUSIONS

This work presented the implementation and experimental validation a control system for an MGC, which comprised separate DC and AC MGs interconnected to a local grid. This system incorporated various types of technologies: the DC MG incorporated DC loads, a WT, an FC, an EZ, and an UC; and the AC MG incorporated AC loads, a BESS, and a PV generator.

The control system consisted of a dynamic centralized EMS which coordinates power distribution while ensuring the correct usage of the ESSs and local device controller. HIL testing was carried out implementing the MGC model and the EMS in an experimental validation environment, mainly composed of an OPAL-RT unit and a Siemens PLC. This approach aimed to verify the performance of the control system using a device with improved reliability and robustness, enabling real-time control and optimization within a PLC commonly used in industrial environments. While the HIL testing in OPAL-RT does not fully capture the complexities of a real MG, it allowed to implement and verify the behavior of the control system in real-time.

The dynamic centralized EMS was tested under different scenarios of fluctuating incident solar radiation and wind speed, and dynamic loads conditions to evaluate its performance in the experimental validation environment. The results exhibited robust performance across them, achieving minimal power exchange with the local grid and fulfilling the objectives set by the dynamic EMS. Therefore, the dynamic EMS can adapt to real-time changes in renewable generation and load demand, which is essential for practical applications. Additionally, the successful implementation and verification of the control system with equipment used in industrial environments is a key contribution, demonstrating the practical applicability of the proposed solution. This highlights the robustness and effectiveness of the proposed control system for MGCs.

Future work could investigate an hierarchical control architecture, with individual MG EMSs implemented in a dedicated PLCs/microcontrollers overseen by a higher-level cluster EMS. This approach may offer increased scalability and resilience for larger and more complex MGCs.

REFERENCES

[1] E. Rosales-Asensio, D. B. Diez, P. Cabrera, and P. Sarmento, "Effectiveness and efficiency of support schemes in promoting renewable energy sources in the Spanish electricity market," *International Journal of Electrical Power & Energy Systems*, vol. 158, p. 109926, Jul. 2024, doi: 10.1016/J.IJEPES.2024.109926.

[2] A. Chebabhi, I. Tegani, A. D. Benhamadouche, and O. Kraa, "Optimal design and sizing of renewable energies in microgrids based on financial considerations a case study of Biskra, Algeria," *Energy Convers Manag*, vol. 291, p. 117270, Sep. 2023, doi: 10.1016/J.ENCONMAN.2023.117270.

[3] A. C. B. Monteiro, R. P. França, R. Arthur, and Y. Iano, "Overview of microgrids in the modern digital age: an introduction and fundamentals," *Residential Microgrids and Rural Electrifications*, pp. 27–43, Jan. 2022, doi: 10.1016/B978-0-323-90177-2.00011-6.

[4] R. Wang *et al.*, "Technology standards for direct current microgrids in buildings: A review," *Renewable and Sustainable Energy Reviews*, vol. 211, p. 115278, Apr. 2025, doi: 10.1016/J.RSER.2024.115278.

[5] Pragya and R. Thakur, "A Review of Architecture and Control Strategies of Hybrid AC/DC Microgrid," *2022 International Conference on Intelligent Controller and Computing for Smart Power, ICICCSP 2022*, 2022, doi: 10.1109/ICICCSP53532.2022.9862386.

[6] W. Dong *et al.*, "Stochastic optimal scheduling strategy for a campus-isolated microgrid energy management system considering dependencies," *Energy Convers Manag*, vol. 292, p. 117341, Sep. 2023, doi: 10.1016/J.ENCONMAN.2023.117341.

[7] G. Zhao, J. Luo, N. Song, and J. Shu, "Multi-objective optimal dispatch of island microgrid considering a novel scheduling resource," *Electric Power Systems Research*, vol. 241, p. 111378, Apr. 2025, doi: 10.1016/J.EPSR.2024.111378.

[8] A. Nawaz *et al.*, "MPC-driven optimal scheduling of grid-connected microgrid: Cost and degradation minimization with PEVs integration," *Electric Power Systems Research*, vol. 238, p. 111173, Jan. 2025, doi: 10.1016/J.EPSR.2024.111173.

[9] B. Chen, J. Wang, X. Lu, C. Chen, and S. Zhao, "Networked Microgrids for Grid Resilience, Robustness, and Efficiency: A Review," Jan. 01, 2021, *IEEE Transactions on Smart Grid.* doi: 10.1109/TSG.2020.3010570.

[10] T. Sattarpour, S. Golshannavaz, D. Nazarpour, and P. Siano, "A multi-stage linearized interactive operation model of smart distribution grid with residential microgrids," *International Journal of Electrical Power & Energy Systems*, vol. 108, pp. 456–471, Jun. 2019, doi: 10.1016/J.IJEPES.2019.01.023.

[11] A. R. Abbasi and D. Baleanu, "Recent developments of energy management strategies in microgrids: An updated and comprehensive review and classification," *Energy Convers Manag*, vol. 297, p. 117723, Dec. 2023, doi: 10.1016/J.ENCONMAN.2023.117723.

[12] M. A. Hasan and S. K. Parida, "An overview of solar photovoltaic panel modeling based on analytical and experimental viewpoint," *Renewable and Sustainable Energy Reviews*, vol. 60, pp. 75–83, Jul. 2016, doi: 10.1016/J.RSER.2016.01.087.

[13] A. Yazdani and I. Reza, *Voltage source converter in power system*. 2010. Accessed: Jul. 28, 2023. [Online]. Available: https://www.wiley.com/en-ca/Voltage+Sourced+Converters+in+Power+Systems+%3A+Modeling%2C+Control%2C+and+Applications-p-9780470521564

[14] R. Sarrias-Mena, L. M. Fernández-Ramírez, C. A. García-Vázquez, and F. Jurado, "Electrolyzer models for hydrogen production from wind energy systems," *Int J Hydrogen Energy*, vol. 40, no. 7, pp. 2927–2938, Feb. 2015, doi: 10.1016/J.IJHYDENE.2014.12.125.

[15] "Real-Time Simulation Communication Protocols | OPAL-RT," 2024 - OPAL-RT TECHNOLOGIES, Inc. Accessed: Jan. 29, 2025. [Online]. Available: https://www.opal-rt.com/software-communication-protocols/

[16] "Modbus Master - OPAL-RT - Communication Protocol," 2022 - OPAL-RT TECHNOLOGIES, Inc. Accessed: Nov. 05, 2024. [Online]. Available: https://www.opal-rt.com/software-communication-protocols/modbus-master/